

# Identification of *N*-Glycolylneuraminic Acid-containing Gangliosides of Cat and Sheep Erythrocytes

<sup>252</sup>Cf FISSION FRAGMENT IONIZATION MASS SPECTROMETRY IN THE ANALYSIS OF GLYCOSPHINGOLIPIDS\*

(Received for publication, March 3, 1988)

Koichi Furukawa‡, Brian T. Chait§, and Kenneth O. Lloyd‡

From the ‡Sloan-Kettering Institute and §The Rockefeller University, New York, New York 10021

A number of gangliosides were isolated from cat and sheep erythrocytes for use in analyzing the specificity of a panel of human anti-heterophile monoclonal antibodies. The structures of these compounds were determined by a combination of different procedures, including sugar analysis, glycosidase treatment, periodate oxidation, TLC immunostaining, methylation analysis, and mass spectrometry. These methods identified the cat erythrocytes gangliosides (C1 and C2) as *N*-glycolylneuraminic acid (NeuGc)-containing hematosides; C1 was shown to be NeuGcα2→8NeuGcα2→3Galβ1→4Glc-Cer ((NeuGc)<sub>2</sub>G<sub>D3</sub>) and C2 to be NeuAcα2→8NeuGcα2→3Galβ1→4Glc-Cer ((NeuAc-NeuGc-)G<sub>D3</sub>). The two sheep gangliosides (S1 and S2) were found to be novel glycolipids based on the paragloboside sequence; S1 was identified as NeuGcα2→8NeuGcα2→3Galβ1→4GlcNAcβ1→3Galβ1→4Glc-Cer ((NeuGc)<sub>2</sub>-disialylparagloboside) and S2 as NeuAcα2→8NeuGcα2→3Galβ1→4GlcNAcβ1→3Galβ1→4Glc-Cer ((NeuAc-NeuGc-)-disialylparagloboside). Structural analysis of these compounds was aided by the use of <sup>252</sup>Cf fission fragment ionization time-of-flight mass spectrometry. This method provided easily interpretable spectra on methylated derivatives which were particularly useful in determining the sialic acid composition of the gangliosides and the sequence of their disialosyl side chains.

Gangliosides have been isolated and characterized from the erythrocytes of a number of animal species. The nature of the gangliosides varies considerably between different species (reviewed in Ref. 1). For example, in man *N*-acetylneuraminic acid-type (NeuAc)<sup>1</sup> sialylparagloboside is the major ganglio-

side (2), in bovine erythrocytes *N*-glycolylneuraminic acid-type G<sub>M3</sub> and NeuGc-sialylparagloboside are the major forms (3, 4), and erythrocytes of European dogs contain exclusively (NeuAc)G<sub>M3</sub> (5). In some animal species the gangliosides have entirely NeuAc-containing gangliosides (*e.g.* man) while other species have entirely or mostly NeuGc-containing gangliosides.

In the process of analyzing the specificity of a panel of human monoclonal antibodies (6), we noted that two of them (2-39M and 32-27M) reacted with gangliosides present in non-human animal erythrocytes, including cat and sheep erythrocytes. In this communication we describe the isolation and structure determination of two gangliosides from cat erythrocytes and two from sheep erythrocytes which react with Ab32-27M. Cat erythrocytes have previously been shown to contain (NeuGc)<sub>2</sub>G<sub>D3</sub> as their major ganglioside (7) and to have a number of minor species, including one which was partially characterized as (NeuAc-NeuGc-)G<sub>D3</sub> (8). We have now determined the structure of the two cat gangliosides in more detail and have also demonstrated the structure of two novel gangliosides from sheep erythrocytes, which unlike the cat gangliosides are based on paragloboside sequences. In the course of studying these structures we utilized <sup>252</sup>Cf fission fragment ionization mass spectrometry to analyze methylated gangliosides. This technique, which apparently has not been used previously in the glycosphingolipid field, gave valuable information on the structures of these compounds.

## EXPERIMENTAL PROCEDURES<sup>2</sup>

**Materials**—G<sub>D3</sub><sup>3</sup> was isolated from human melanoma cells as described previously (9). (NeuAc)G<sub>M3</sub> was purified from dog erythrocytes as described by Yasue *et al.* (5), and (NeuGc)G<sub>M3</sub> was obtained from horse erythrocytes (10); their structures were confirmed by compositional and methylation analysis. G<sub>M1</sub> was purchased from Supelco Inc., Bellefonte, PA. Cat blood was obtained from Cocalico Biologicals, Inc., Reamstown, PA, and sheep blood was obtained from Pel-Freez Biologicals, Rogers, AR. Mouse monoclonal antibodies to lacto-*N*-tetraosylceramide (K21, Ref. 11) and to lacto-*N*-neotetraosylceramide (1B2, Ref. 12) have been described; the latter was kindly provided by Dr. S. Hakomori. The human monoclonal antibodies have also been described (6).

**Immunochemical Methods**—Immunostaining on TLC plates was performed using aluminum-backed plates (E. Merck, West Germany) as reported (13).

\* This work was supported by Grant IM-429 from the American Cancer Society and by Grants CA 08478 and CA 47427 from the National Institutes of Health. The Rockefeller University Mass Spectrometric Biotechnology Research Resource is supported by the Division of Research Resources, National Institutes of Health (Grant RR-00862-14). The costs of publication of this article were defrayed in part by the payment of page charges. This article must therefore be hereby marked "advertisement" in accordance with 18 U.S.C. Section 1734 solely to indicate this fact.

<sup>1</sup> The abbreviations used are: NeuAc, *N*-acetylneuraminic acid; NeuGc, *N*-glycolylneuraminic acid; GC, gas chromatography; MS, mass spectrometry; TLC, thin layer chromatography; mAb, monoclonal antibody; FAB, fast atom bombardment spectrometry. Ganglioside nomenclature is based on that of Svennerholm (39): G<sub>M3</sub>, NeuAc (or NeuGc)α2→3Galβ1→4Glc-Cer; G<sub>D3</sub>, NeuAc (or NeuGc)α2→8NeuAc (or NeuGc)α2→3Galβ1→4Glc-Cer; G<sub>M1</sub>, Galβ1→3GalNAcβ1→4(NeuAcα2→3)Galβ1→4Glc-Cer. Other glycolipids were: paragloboside (lacto-*N*-neotetraosylceramide), Galβ1→4GlcNAcβ1→3Galβ1→4Glc-Cer; lacto-*N*-tetraosylceramide, Galβ1→3GlcNAcβ1→3Galβ1→4Glc-Cer.

<sup>2</sup> Portions of this paper (including part of "Experimental Procedures," part of "Results," Figs. 1, 2, 9, 15-17, and Table III) are presented in miniprint at the end of this paper. Miniprint is easily read with the aid of a standard magnifying glass. Full size photocopies are included in the microfilm edition of the Journal that is available from Waverly Press.

<sup>3</sup> When not otherwise indicated, gangliosides contain *N*-acetylneuraminic acid.

**Extraction and Purification of Gangliosides**—Animal erythrocytes were lysed in hypotonic solution and the membranes isolated as described (13). The dried membranes were extracted in chloroform-methanol (2:1, 1:1, and 1:2 successively), and the glycolipid fraction was isolated by Florisil column chromatography on acetylated derivatives according to Saito and Hakomori (14). Neutral glycolipids were separated from gangliosides on a DEAE-Sephadex column (A50, Pharmacia LKB Biotechnology Inc.), and the gangliosides were eluted with chloroform, methanol, 0.8 M ammonium acetate (15). The sheep gangliosides were further fractionated by stepwise elution from a DEAE-Sephadex column with chloroform:methanol:ammonium acetate (30:60:8) containing 0.05, 0.1, 0.15, 0.2, 0.25, 0.3, 0.4, 0.6, and 0.8 M salt. The two major disialogangliosides appeared in the 0.2 and 0.25 M salt fractions. The sheep and cat erythrocyte gangliosides were further purified by preparative TLC on Silica Gel G plates (Fisher). During the fractionation, the reactivity with human mAbs was followed by enzyme-linked immunosorbent assay and/or immunostaining procedures. The isolated gangliosides were checked for purity in three solvent systems: chloroform:methanol:water, 60:35:8 (solvent 1); chloroform, methanol, 2.5 N ammonia, 60:35:8 (solvent 2); and 1-propanol:ammonia:water, 60:9.5:11.5 (solvent 3). Gangliosides were visualized with resorcinol spray.

**Analytical Procedures**—Sugar components in the gangliosides were analyzed after methanolysis and trifluoroacetylation as described by Zanetta *et al.* (16) using a Perkin-Elmer gas chromatograph model 8400 and 5% SP-2401 on a 100/200 Supelcoport column (Supelco, Inc.). Sialic acid levels were determined using the thiobarbituric acid method (17). Sialic acid composition (NeuAc and NeuGc) was analyzed after methanolysis and trimethylsilylation by Hydrox-Sil (Regis Chemical Co.) as described by Yu and Ledeen (18) using a 3% OV-1 on a 100/200 Supelcoport column. Fatty acid composition was determined by methanolysis in 1.0 N methanolic HCl at 80 °C for 18 h and separation of the methyl esters on a 3% OV-1 column.

**Neuraminidase Treatment**—The effect of both partial and complete neuraminidase treatment was determined. The sample (2 µg) was sonicated in 20 µl of sodium acetate buffer, 0.1 M, pH 4.9. Neuraminidase (*Vibrio cholerae*, Calbiochem, 0.3 IU) was added, and the sample was incubated for 30 min at 30 °C (partial hydrolysis). Another sample, treated under the same conditions, was incubated for 120 min at 37 °C (complete hydrolysis).

**Periodate Oxidation**—Periodate-borohydride treatment to determine the order and substitution of sialic acid residues in the gangliosides was performed according to Ando and Yu (19). Ganglioside (20 µg) was dissolved in 135 µl of 0.2 M sodium acetate buffer (pH 4.4), and 15 µl of 0.5 M sodium periodate was added. After incubation for 18 h at 4 °C, 25 µl of 10 M ethylene glycol was added to stop the reaction. After 3 h, 45 µl of 0.2 N NaOH was added to adjust the pH to about 6.5. Sodium borohydride (30 µl of 9%) was added at 0 °C and after incubation overnight at 4 °C, 35 µl of 2 M acetic acid was added. The sample was finally desalted on a C18 cartridge (Waters-Millipore, Medford, MA) and analyzed for its sialic acid content by gas chromatography as described above.

**Permethylated Analysis**—Permethylated gangliosides were performed according to the Hakomori procedure (20) with slight modification. Gangliosides (50–200 µg) were dissolved in dimethyl sulfoxide (100 µl) and sonicated for 1 h. Methylsulfanylcarbanion solution (100 µl) was then added, and the sample was sonicated for 1 h. After checking for the presence of excess reagent with triphenylmethane, methyl iodide (150 µl) was added slowly, and the mixture was stirred for 2 h at room temperature. The reaction was terminated by adding water, and the permethylated derivatives were isolated by C18 reverse phase chromatography on a Sep-Pak cartridge (Waters-Millipore). They were further purified by preparative TLC on silica gel plates in chloroform:methanol (90:5) solvent.

For analysis of neutral and amino sugars, permethylated gangliosides were hydrolyzed with 150 µl of 0.5 N H<sub>2</sub>SO<sub>4</sub> in 95% acetic acid at 80 °C for 18 h; water (150 µl) was then added, and hydrolysis was continued for 5 more h. After passing the sample through a Dowex 1 (X8) column (acetate form), fatty acids were extracted with *n*-hexane. The samples were then reduced with sodium borodeuteride (30 mg/ml), neutralized with acetic acid in methanol, and dried. The samples were analyzed by GC-MS (21, 22) on a 5% phenylmethyl silicone capillary column and a temperature gradient from 120 to 250 °C at 10 °C/min. The mass spectrometer used was a VG 70-250 double magnetic focusing deflection instrument coupled to an HP 5790A gas chromatograph. Both electron impact (EI) and chemical ionization spectra (CI) were collected.

For analysis of sialic acids (23), methylated gangliosides were

methanolized in 0.05 N HCl in methanol or 0.5 N HCl in methanol for 5 or 18 h, respectively. After removal of the fatty acids with hexane, the samples were acetylated with pyridine and acetic anhydride. Methanol was then added, and the sample was dried. A mixture of chloroform:methanol:H<sub>2</sub>O was added, and after mixing and centrifuging, the lower layer was removed and dried. The sample was analyzed by gas chromatography on a packed 3% OV-1 column at 210 °C or on a SPB-5 wide bore capillary column (30 m × 0.35 mm). The samples were also analyzed by GC/MS as described above.

<sup>252</sup>Cf Fission Fragment Ionization Mass Spectrometry—<sup>252</sup>Cf fission fragment ionization mass spectrometry conditions are described in the Miniprint Supplement.

## RESULTS

Cat erythrocyte membranes contain one major and a number of minor ganglioside species. Fractionation of the gangliosides from 2.2 g (dry weight) of membranes as described under "Experimental Procedures" yielded 1200 µg of the major ganglioside (C1) and 180 µg of another ganglioside (C2), both of which were selected on the basis of their reactivity with human mAb 32-27M (Fig. 1). Sheep membranes yielded two major gangliosides both of which reacted with mAb 32-27M (Fig. 2). From 13.0 g (dry weight) of sheep erythrocyte membranes, 120 µg of ganglioside S1 and 270 µg of ganglioside S2 were isolated and purified (Fig. 2).

**Compositional, Chemical, and Immunochemical Analysis of Gangliosides**—The two cat erythrocyte gangliosides (C1 and C2) contained galactose, glucose, and sialic acid in approximate ratios of 1:1:2 but no *N*-acetylglucosamine or *N*-acetylgalactosamine (Table I). Further analysis of the sialic acid showed that C1 contained almost entirely (98%) NeuGc and C2 had NeuGc and NeuAc in an approximately 1:1 ratio (Table 1). Preliminary data indicating the presence of disialyl chains and the sequence of their sialic acid residues were obtained by analyzing the susceptibility of the sugars to periodate oxidation (19). In glycolipid C1, NeuGc remained after periodate oxidation indicating the presence of disialyl-NeuGc-NeuGc- sequences (Table I). In glycolipid C2, all the NeuAc was destroyed after periodate treatment and NeuGc remained; this result is consistent with a NeuAc-NeuGc-sequence. Treatment of the C1 and C2 with neuraminidase converted them to products migrating with (NeuGc)<sub>G<sub>M3</sub></sub> (Fig. 3B) and lactosylceramide (Fig. 3C). The former reacted with mAb 2-39M, thus confirming its identity as (NeuGc)<sub>G<sub>M3</sub></sub> (Fig. 3B).

Both sheep glycolipids S1 and S2 were shown to contain glucose, galactose, *N*-acetylglucosamine, and sialic acid in the approximate ratio of 1:2:1:2 (Table I). Further analysis of the sialic acids demonstrated that S1 contained about 90% of NeuGc, whereas S2 had both NeuGc and NeuAc in a ratio of 1:1 (Table I). Periodate treatment indicated the presence of disialyl NeuGc-NeuGc- sequences in S1 and NeuAc-NeuGc-sequences in S2 (Table I). Neuraminidase treatment of both

TABLE I  
Carbohydrate composition of cat and sheep erythrocyte gangliosides and effect of periodate treatment

Sam- ple	Ratios				Sialic acids				
					Original		After periodate		
	Glc	Gal	GlcNAc	GalNAc	Sialic acid	NeuAc	NeuGc	NeuAc	NeuGc
					% <sup>a</sup>		% <sup>a</sup>		
C1	1.00	1.09	0	0	1.94	1.7	98.3	0	100
C2	1.00	1.17	0	0	1.66	34.0	66.0	1.0	99.0
S1	1.00	1.90	1.11	0	1.96	9.8	90.2	3.6	96.4
S2	1.00	2.14	1.05	0	2.02	47.8	52.2	6.7	96.4

<sup>a</sup> As percentage of total sialic acid.

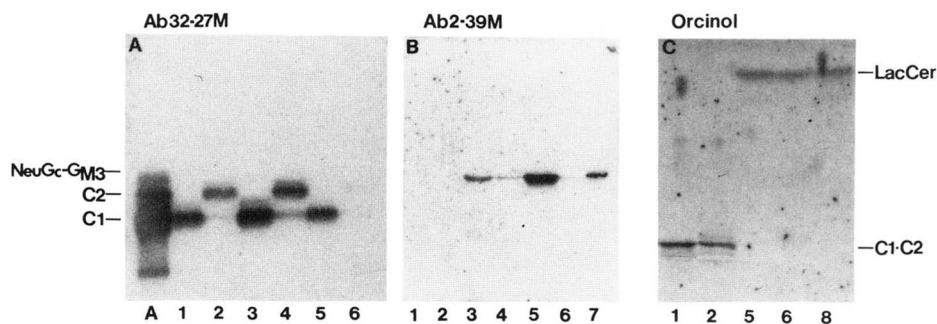


FIG. 3. Neuraminidase treatment of cat gangliosides. Panel A, reactivity of treated and untreated samples with mAb 32-27M (reacting with C1 and C2). Panel B, reactivity with mAb 2-39M (reacting with NeuGc-G<sub>M3</sub>). Panel C, orcinol HCl-sprayed plate. Lane 1, C1; lane 2, C2; lane 3, C1 treated with neuraminidase (30 °C for 30 min); lane 4, C2 treated with neuraminidase (30 °C for 30 min); lane 5, C1 treated with neuraminidase at 37 °C for 120 min; lane 6, C2 treated with neuraminidase at 37 °C for 120 min; lane 7, NeuGc-G<sub>M3</sub>; lane 8, lactosylceramide (LacCer); A, unfractionated cat erythrocyte gangliosides. Solvent for A and B, solvent 2; solvent for C, solvent 1.

gangliosides resulted in the formation of a new glycolipid reacting with a monoclonal antibody directed to Galβ1→4GlcNAcβ1→3Galβ1→4Glc-Cer (paragloboside) (Fig. 4B) but not with an antibody reacting with Galβ1→3GlcNAcβ1→3Galβ1→4Glc-Cer (data not shown).

**Methylation Analysis**—The four gangliosides were methylated using the Hakomori procedure (20). For analysis of the hexose and hexosamine derivatives, the samples were hydrolyzed, reduced, and acetylated and analyzed by GC-MS as described by Bjorndal *et al.* (21) and Stellner *et al.* (22). Methylation analysis of the two cat erythrocyte ganglioside samples showed the presence of 2,4,6-tri-*O*-methyl-1,3,5-tri-*O*-acetylgalactitol and 2,3,6-tri-*O*-methyl-1,4,5-tri-*O*-acetylglucitol in each methylated glycolipid (Table II). Methylated derivatives for the neutral sugars from the S1 and S2 gave

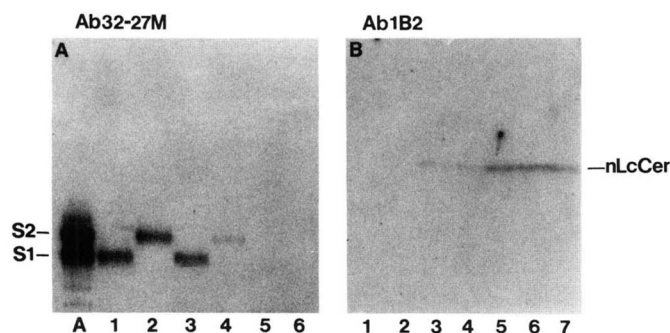


FIG. 4. Neuraminidase treatment of sheep erythrocyte gangliosides. Panel A, reactivity with mAb 32-27M (detecting S1 and S2); panel B, reactivity with mAb 1B2 (detecting lacto-*N*-neotetraosylceramide (nLcCer)). Lane 1, S1; lane 2, S2; lane 3, treatment of S1 with neuraminidase at 30 °C for 30 min; lane 4, treatment of S2 with neuraminidase at 30 °C for 30 min; lane 5, treatment of S1 with neuraminidase at 37 °C for 120 min; lane 6, treatment of S2 with neuraminidase at 37 °C for 120 min; lane 7, lacto-*N*-neotetraosylceramide. A, unfractionated sheep erythrocyte gangliosides. Solvent: 2.

TABLE II

Methylated hexitols and *N*-acetylhexosaminotols identified in hydrolysates of methylated cat and sheep erythrocyte gangliosides by gas chromatography-mass spectrometry

Ganglioside	1,3,5-Tri- <i>O</i> -Ac- 2,4,6-tri- <i>O</i> - Me-Gal	1,4,5-Tri- <i>O</i> -Ac- 2,3,6-tri- <i>O</i> - Me-Glc	1,4,5-Tri- <i>O</i> -Ac- 3,6-di- <i>O</i> -Me- <i>N</i> - Me-GlcNAc
C1	+	+	—
C2	+	+	—
S1	++	+	+
S2	++	+	+

chromatograms that were very similar to each other and showed three main peaks. Chemical ionization spectra (not shown) indicated that the three components were two tri-*O*-methyl-acetylated hexitols and one di-*O*-methyl-*N*-methyl-acetylated hexosaminitol derivatives. Examination of the EI spectra and comparison with published fragmentation patterns identified the three compounds as 2,4,6-tri-*O*-methyl-1,3,5-tri-*O*-acetylgalactitol, 2,3,6-tri-*O*-methyl-1,4,5-tri-*O*-acetylglucitol, and 3,6-di-*O*-methyl-1,4,5-tri-*O*-acetyl-2-deoxy-*N*-methyl-*N*-acetamidoglucitol (Table II).

Analysis of methylated sialic acid derivatives was carried out on *O*-acetylated derivatives after mild methanolysis of the methylated glycolipids. Initially the conditions used for methanolysis were 0.5 N HCl in methanol at 100 °C for 18 h as described by Rauvala and Karkkainen (23). However, under these conditions we observed selective de-*N*-acylation of the *N*-glycolyl group from the internal sialic acid of disialyl glycolipids; the external *N*-acyl group was unaffected. This phenomenon was previously noted by Inoue and Matsumura (24) in their analysis of trout egg glycoprotein. They suggested a nucleophilic attack of the 8-*O* group of the internal sialic acid on the amide carbonyl group of the same sugar as the mechanism for this unexpected reaction.

Subsequent analysis of the sialic acid derivatives from C1, C2, S1, and S2 was therefore carried out using methanolysis in 0.05 N HCl in methanol at 80 °C for 5 h. Analysis of the derivatives by GC-MS (Fig. 5) and measuring both CI and EI spectra demonstrated the nature and arrangement of the sialic acid residues and the position of substitution on the internal sialic acid. *N*-Glycolyl-containing sialic acid derivatives were readily distinguished by giving protonated intact molecule ions in their CI spectra of 30 *m/z* units higher than the corresponding *N*-acetyl derivatives. The EI spectra also showed characteristic fragments 30 mass units higher in the spectra of *N*-glycolyl-containing compounds, for example, prominent fragments were observed at 159 *m/z* for NeuGc and at 129 *m/z* for NeuAc (Fig. 6).

By using these procedures, analysis of the cat ganglioside C1 showed the presence of 1,2,4,7,8,9-hexa-*O*-methyl-*N*-methyl-*N*-glycolylneuraminic acid methyl glycoside and 1,2,4,7,9-penta-*O*-methyl-8-*O*-acetyl-*N*-methyl-*N*-glycolylneuraminic acid methyl ester (Fig. 6). Methylated C2 had the same 8-*O*-acetyl derivative and 1,2,4,7,8,9-hexa-*O*-methyl-*N*-methyl-*N*-acetylneuraminic acid glycoside (Fig. 6). These results show that C1 has a NeuGcα2→8NeuGc side chain, whereas C2 has a NeuAcα2→8NeuGc side chain. A similar analysis of the two sheep erythrocyte glycolipids demon-

FIG. 5. Gas chromatography of *N*- and *O*-methylated *O*-acetylated sialic acid derivatives of sheep and cat gangliosides as their methyl glycosides. Panel A, C1; panel B, C2. Peaks are identified by their scan numbers, and their EI mass spectra are shown in Fig. 6. S1 gave results very similar to C1, and S2 was similar to C2.

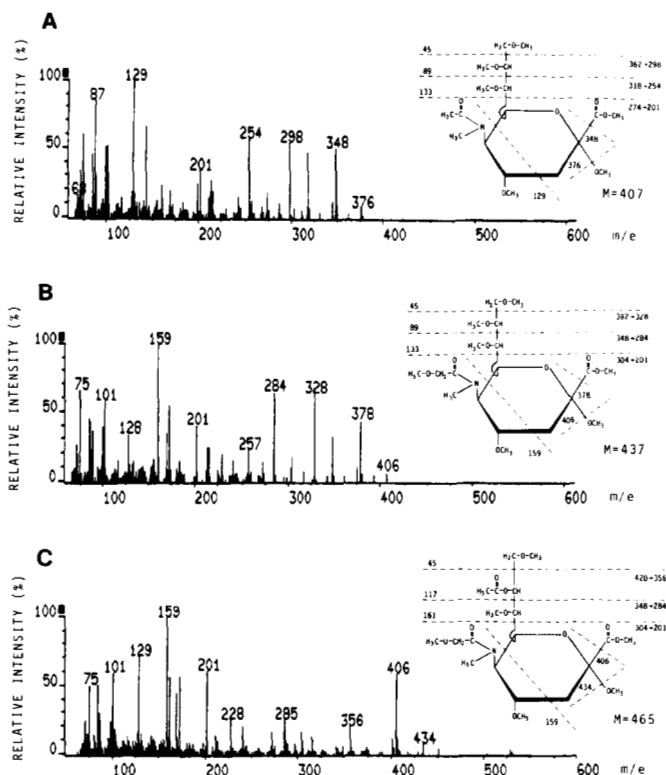
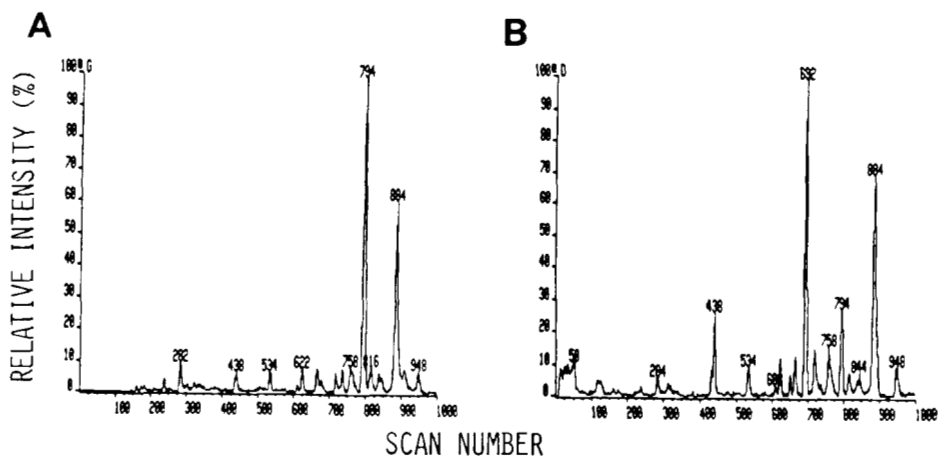


FIG. 6. EI mass spectra of *N*- and *O*-methyl-*O*-acetyl derivatives of sialic acid methyl glycosides obtained from cat and sheep gangliosides. Panel A, spectrum of peak 632 (Fig. 5); panel B, spectrum of peak 794 (Fig. 5); panel C, spectrum of peak 884 (Fig. 5). Fragmentation patterns for the three sugars are also shown.

stated that S1 also has NeuGca2→8NeuGc side chains and S2 has NeuAca2→8NeuGc units.

<sup>252</sup>Cf Fission Fragment Ionization Mass Spectrometry of Methylated Gangliosides—Mass spectrometric analysis using <sup>252</sup>Cf fission fragment ionization produced a significant amount of detailed information on the structures of the cat and sheep erythrocyte glycolipids. Since this technique has not been used previously in analyzing glycosphingolipids, a number of model gangliosides of known structure were first studied. These were (NeuAc)<sub>2</sub>G<sub>M1</sub>, (NeuAc)<sub>2</sub>G<sub>M3</sub>, (NeuGc)<sub>2</sub>G<sub>M3</sub>, and (NeuAc)<sub>2</sub>G<sub>D3</sub>. The results of this study on model gangliosides are presented in the Miniprint Supplement.

Once the systematics of the fission fragment ionization-induced fragmentation of the standard gangliosides were established, application of this method to the methylated gangliosides from cat and sheep erythrocytes readily yielded

information on their structures. The mass spectrum of ganglioside C1 (Fig. 7), thought from previously discussed data to be (NeuGc)<sub>2</sub>G<sub>D3</sub>, was clearly consistent with this structure (Fig. 8, where R<sub>1</sub> = R<sub>2</sub> = CH<sub>3</sub>OCH<sub>2</sub>CO-). The major quasi-molecular ion arising from sodium ion addition to the intact C1 molecule observed at *m/z* 1905 was 60 mass units higher than the corresponding component from (NeuAc)<sub>2</sub>G<sub>D3</sub> observed at *m/z* 1845 (Fig. 9). This difference corresponds to the substitution of *N*-glycolyl groups in place of the *N*-acetyl groups. This interpretation is borne out by the presence of the peak at *m/z* 797 in the spectrum of C1 (Fig. 7) corresponding to ((NeuGc-NeuGc-) + H<sup>+</sup>-H), the peak at *m/z* 777 corresponding to ((NeuGc-NeuGc-) + Na<sup>+</sup>-COOCH<sub>3</sub>), and the prominent NeuGc-derived peaks at *m/z* 406 (A + H<sup>+</sup>-OH) and *m/z* 374 (A + H<sup>+</sup>-CH<sub>3</sub>OH). Additional fragment ions arising from cleavages at *D*, *E*, *F*, and *G* (Fig. 8) complete the sequence characterization of the carbohydrate portion of C1. Information regarding the ceramide portion of C1 is derived from three groups of spectral peaks. The weak group centered at about *m/z* 1651, which we attribute to cleavage between C2 and C3 of the base (*J* + Na<sup>+</sup>-H), indicates the base to be largely 4-sphingenine. The (*Y* + H<sup>+</sup>-H) ceramide group centered about the dominant *m/z* 659 and 661 peaks then provide information on the distribution of the various fatty acyl components of C1; the two main components were C24:1 and C24:0. Finally the heterogeneity observed in the *Y* ceramide fragment ion peaks is observed to be largely mirrored in the group of peaks corresponding to the sodium-cationized intact C1 molecule designated (*M* + Na<sup>+</sup>). The other cat erythrocyte ganglioside C2 yielded a dominant (*M* + Na<sup>+</sup>) ion at *m/z* 1875 (Fig. 10) consistent with the molecule containing 2 hexose units, one NeuAc, one NeuGc, and a ceramide with mainly C24:0 and C24:1 fatty acyl chains. Not only did the spectrum contain peaks at *m/z* 767 (*B* + H<sup>+</sup>-H) and at *m/z* 747 (*C* + Na<sup>+</sup>-COOCH<sub>3</sub>) derived from a disialyl unit but also intense peaks at *m/z* 376 (A + H<sup>+</sup>-H) and *m/z* 344 (A + H<sup>+</sup>-H-CH<sub>3</sub>) derived from a NeuAc unit (Fig. 8 where R<sub>1</sub> = CH<sub>3</sub>CO-, R<sub>2</sub> = CH<sub>3</sub>OCH<sub>2</sub>CO-). The presence of these latter peaks, rather than the corresponding NeuGc-derived peaks expected at *m/z* 406 and 374, clearly confirms the order of the sugars to be NeuAc-NeuGc- as deduced from the methylation data.

The mass spectra of the two sheep gangliosides could be similarly interpreted. Methylated sheep ganglioside S1 gave an (*M* + Na<sup>+</sup>) at *m/z* 2355 (Fig. 11), consistent with the molecule containing 3 hexose units, 2 NeuGc units, and a ceramide with mainly C24 fatty acyl chains. In addition to fragments ions derived from NeuGc and NeuGc-NeuGc-, fragments at *m/z* 993, 1010, and 1040 derived from the terminal

FIG. 7.  $^{252}\text{Cf}$  fission fragment ionization time-of-flight mass spectrum of methylated cat erythrocyte ganglioside C1. The region between  $m/z$  300 and 2300 is shown.  $M$  designates the intact molecule. The labels on the fragment ion peaks refer to the fragmentation sites indicated in Fig. 8 where  $R = \text{CH}_3$ .

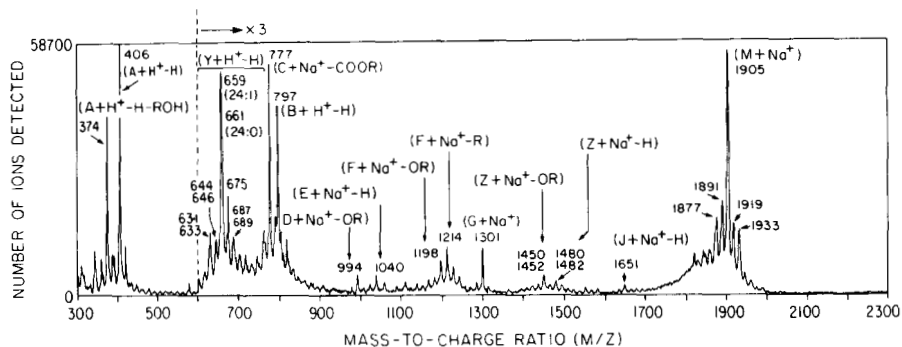


FIG. 8. Structure of  $\text{G}_{\text{D3}}$  showing proposed fragmentation pattern in fission fragment MS.

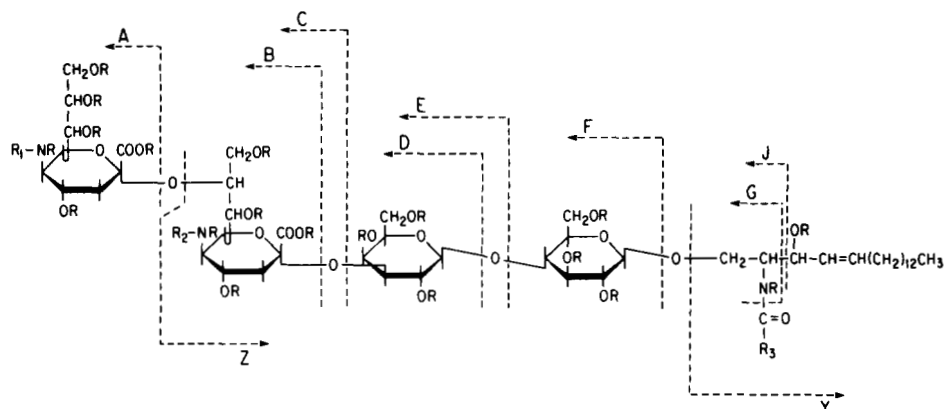


FIG. 10. Mass spectrum of methylated cat erythrocyte ganglioside C2. The region between  $m/z$  300 and 2300 is shown.  $M$  designates the intact molecule. The labels on the fragment ions peaks refer to the fragmentation sites indicated in Fig. 8 where  $R = \text{CH}_3$ .  $i$  indicates ions originating from impurities.

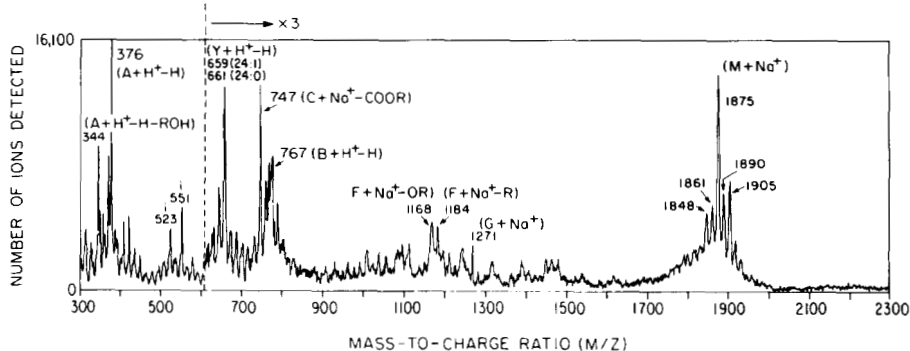
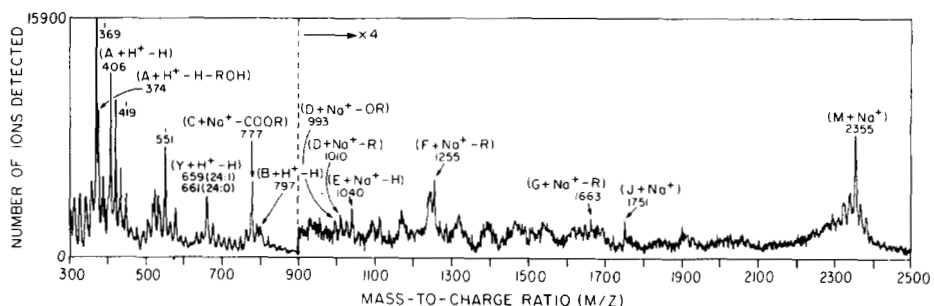


FIG. 11. Mass spectrum of methylated sheep erythrocyte ganglioside S1. The region between  $m/z$  300 and 2500 is shown.  $M$  designates the intact molecule. The labels on the fragment ion peaks refer to the fragmentation sites indicated in Fig. 12 where  $R = \text{CH}_3$ .  $i$  indicates impurity ions.



trisaccharide, NeuGc-NeuGc-Gal- (fragments  $D$  and  $E$  in Fig. 12 where  $R_1 = R_2 = \text{CH}_3\text{OCH}_2\text{CO}-$ ), and a fragment at  $m/z$  1255 derived from the terminal tetrasaccharide, NeuGc-NeuGc-Gal-GlcNAc-, confirmed the site of substitution of the disialyl unit and the sequence of the sugars. Methylated sheep ganglioside S2 gave an  $(M + \text{Na}^+)$  at  $m/z$  2325 (Fig. 13) consistent with a similar composition as S1, including C24 fatty acids, except for the substitution of a NeuAc residue for one of the NeuGc residues (leading to a difference of 30 mass units). Other particularly significant features of this spectrum were peaks at  $m/z$  767 and 747 derived from the disialyl group

containing one NeuAc and one NeuGc residue and also intense peaks at  $m/z$  376 and 344. The presence of the latter two peaks indicates that NeuAc is the terminal residue. This confirms the methylation data in assigning a NeuAc-NeuGc-sequence to this ganglioside. Again peaks arising from the terminal trisaccharide ( $m/z$  964 and 1010) and the terminal tetrasaccharide ( $m/z$  1225) are present in the spectrum. In summary, these spectra demonstrate the sugar and ceramide composition of the gangliosides. They also provide sequence data, particularly on the sialic acid and other terminal residues. The method was particularly valuable in distinguishing

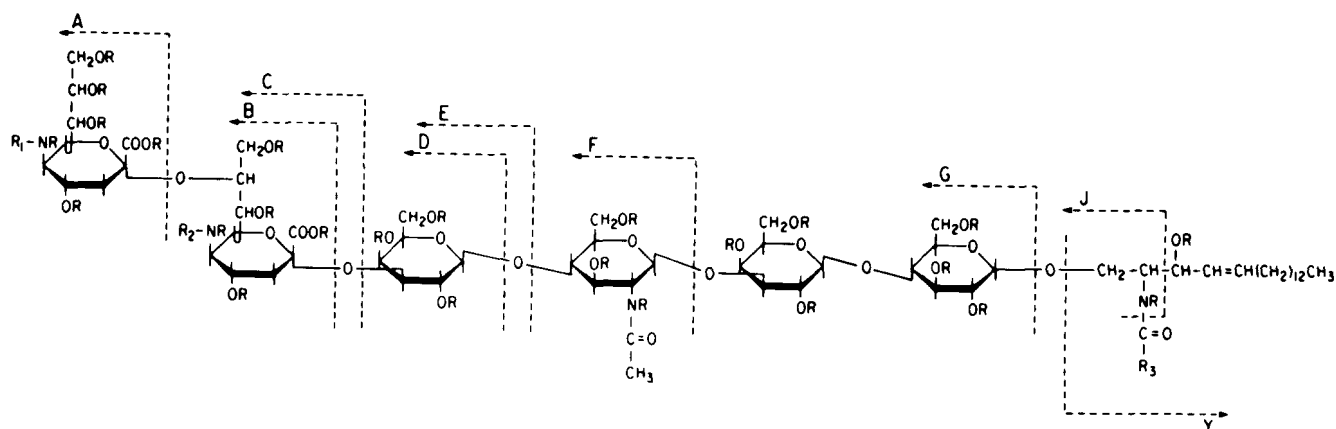
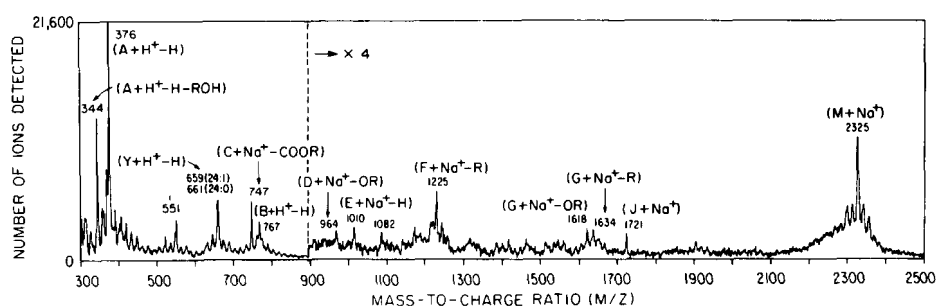


FIG. 12. Structure of disialylparagloboside showing proposed fragmentation pattern in fission fragment MS.

FIG. 13. Mass spectrum of methylated sheep erythrocyte ganglioside S2. The region between  $m/z$  300 and 2500 is shown.  $M$  designates the intact molecule. The labels on the peaks refer to the fragmentation sites indicated in Fig. 12 where  $R = \text{CH}_3$ .  $i$  designates impurity ions.



C1	NeuGca2+8NeuGca2+3Galβ1+4G1c-Cer
C2	NeuAca2+8NeuGca2+3Galβ1+4G1c-Cer
S1	NeuGca2+8NeuGca2+3Galβ1+4G1cNAcβ1+3Galβ1+4G1c-Cer
S2	NeuAca2+8NeuGca2+3Galβ1+4G1cNAcβ1+3Galβ1+4G1c-Cer

FIG. 14. Proposed structures of cat and sheep erythrocyte gangliosides.

between *N*-acetyl- and *N*-glycolylsialic acid substitution and in determining their order in disialogangliosides. In addition the method proved useful in partially characterizing the heterogeneity observed in the ceramide portion of the gangliosides.

**Structures of Gangliosides**—Based on the various procedures used in this study, the structures of the cat and sheep erythrocyte gangliosides can be assigned as shown in Fig. 14. The two cat species are hematosides with di-NeuGc and NeuAc-NeuGc- substituents. The two sheep gangliosides, on the other hand, are based on paragloboside (lacto-*N*-neotetraose) sequences with the same two disialyl substituents as in the cat gangliosides. All four gangliosides have ceramide moieties containing 4-sphinganine and mainly C24:1 and C24:0 fatty acids.

#### DISCUSSION

Two novel gangliosides were isolated from sheep erythrocytes in this study. Although both NeuAc- and NeuGc-sialylparagloboside (3, 4, 25) as well as di-NeuAc-sialylparagloboside (26) have previously been reported, this is the first description of di-NeuGc- and NeuAc-NeuGc-containing disialylparaglobosides. These two species are the major gangliosides of sheep erythrocytes. The isolation of di-NeuGc- $G_{D3}$  as the major ganglioside of cat erythrocytes confirms the work

of Hamanaka *et al.* (7); we also fully analyzed the structure of (NeuAc-NeuGc-) $G_{D3}$  which had previously been reported (8) as another possible ganglioside of cat erythrocytes. Gangliosides containing "mixed" NeuAc/NeuGc sialic acid structures have been previously described, but they are relatively uncommon.

Depending on the species, animal erythrocytes have either ganglio-series (mainly hematosides) or neolacto-series gangliosides as their major acid glycosphingolipids. These gangliosides may contain either NeuAc or NeuGc or both types of sialic acids, and in some animals *O*-acetyl derivatives are also found. The reason for this interspecies variation is unknown. To some extent this composition is phylogenetically determined since erythrocytes from closely related species have similar ganglioside compositions, *e.g.*, members of the *Felidae*, cats, lions, and hyenas, have  $G_{D3}$  as their major erythrocyte ganglioside (1). On the other hand, different inbred strains of mice differ quite considerably in their erythrocyte ganglioside patterns (1).

Our analysis of the small amounts of gangliosides isolated from sheep and cat erythrocytes was greatly aided by the application of  $^{252}\text{Cf}$  fission fragment ionization mass spectrometry. In this method molecules are desorbed and ionized directly from a solid surface by the passage of an energetic fission fragment from  $^{252}\text{Cf}$  through a surface coated with the sample (27). This technique provided spectra with large molecular mass ions and simple easily interpretable fragment ion patterns of the methylated gangliosides. Several other MS methods have been used in obtaining molecular weight and structural information on both derivatized and underivatized samples of intact gangliosides. These include field desorption-MS (28), direct chemical ionization-MS (29), liquid secondary ionization-MS (30), and FAB-MS (30-38). Our results with  $^{252}\text{Cf}$  fission fragment ionization-MS compare most closely with the results obtained on methylated gangliosides using

positive ion FAB-MS (34–38). The spectra bear a close resemblance with respect to the general fragmentation processes which occur. There are, however, several differences in detail. 1) Unlike FAB (and also the other MS techniques), the fission fragment method is essentially nondestructive so that the sample may be reused after the mass spectrometric analysis for further studies. 2) In the FAB technique the sample is suspended in a solvent with low volatility, e.g., glycerol or thioglycerol, which can on occasion interact with the sample to form adduct ions or produce an unwanted background (34, 36). Complications of this kind do not arise in the fission fragment technique because the sample is inserted into the mass spectrometer as a solid film. 3) The FAB analyses are performed with magnetic deflection mass analyzers with sufficient resolution to resolve all adjacent ions peaks in the spectra whereas the fission fragment time-of-flight mass analyzer has insufficient resolution to separate adjacent mass ion peaks above  $m/z$  1000. Nevertheless, in the spectra analyzed in this study, this lack of resolution at high masses did not lead to serious ambiguities. 4) In the fission fragment method, both positive and negative ion spectra of underivatized gangliosides were found to be considerably weaker and less structurally informative than those obtained on methylated samples. However, since methylated samples are very often already available from classical methylation analysis, this is not a serious drawback. The FAB-MS method gives useful negative ion mass spectra of underivatized samples (31–36). 5) In the present study the detailed composition of the various ceramide components could not be ascertained in every case from the fission fragment MS alone since fragment ions specifically related to either the fatty acid or base components were not consistently present. This finding is to be contrasted with the findings on NH<sub>4</sub> direct chemical ionization of methylated-reduced glycosphingolipids (30) and also with FAB-MS of methylated derivatives obtained under certain conditions (35–38). It should also be noted that commercial <sup>252</sup>Cf time-of-flight mass spectrometers are less expensive than double-focusing magnetic deflection mass spectrometers with comparable capabilities.

In summary, <sup>252</sup>Cf fission ion fragmentation MS can be considered to be a useful alternative to FAB-MS for the analysis of methylated gangliosides. In general, less than 1 μg of ganglioside was found to be sufficient to produce a mass spectrum using this method. It should be noted, however, that the sensitivity-limiting step in the total analysis is the amount of material that can be conveniently subjected to the methylation procedure and subsequent purification steps.

*Acknowledgments*—We thank Dr. H. Yamaguchi for providing the human monoclonal antibody, Dr. A. Bencsath, Rockefeller University, for providing the GC-MS results, and William T. Doerrler and Tanuja Chaudhary for skillful technical assistance.

#### REFERENCES

1. Yamakawa, T. (1983) *Red Blood Cells of Domestic Mammals* (Agar, N. S., and Board, P. G., eds) pp. 38–53, Elsevier Scientific Publishing Co., Amsterdam
2. Watanabe, K., Powell, M. E., and Hakomori, S. (1979) *J. Biol. Chem.* **254**, 8223–8229
3. Chien, J.-L., Li, S.-C., Laine, R. A., and Li, Y.-T. (1978) *J. Biol. Chem.* **253**, 4031–4035
4. Uemura, K., Yuzawa, M., and Taketomi, T. (1978) *J. Biochem. (Tokyo)* **83**, 463–471
5. Yasue, S., Handa, S., Miyagawa, S., Inoue, J., Hasegawa, A., and Yamakawa, T. (1978) *J. Biochem. (Tokyo)* **83**, 1101–1107
6. Yamaguchi, H., Furukawa, K., Fortunato, S. R., Livingston, P. O., Lloyd, K. O., Oettgen, H. F., and Old, L. J. (1987) *Proc. Natl. Acad. Sci. U. S. A.* **84**, 2416–2420
7. Hamanaka, S., Handa, S., Inoue, J., Hasegawa, A., and Yamakawa, T. (1979) *J. Biochem. (Tokyo)* **86**, 695–698
8. Ando, N., and Yamakawa, T. (1982) *J. Biochem. (Tokyo)* **91**, 873–881
9. Pukel, C. S., Lloyd, K. O., Travassos, L. R., Dippold, W. G., Oettgen, H. F., and Old, L. J. (1982) *J. Exp. Med.* **155**, 1133–1147
10. Handa, S., and Yamakawa, T. (1964) *Jpn. J. Exp. Med.* **34**, 293–304
11. Rettig, W. J., Cordon-Cardo, C., Ng, J. S. C., Oettgen, H. F., Old, L. J., and Lloyd, K. O. (1985) *Cancer Res.* **45**, 815–821
12. Young, W. W., Jr., Portoukalian, J., and Hakomori, S. (1981) *J. Biol. Chem.* **256**, 10967–10972
13. Furukawa, K., Clausen, H., Hakomori, S., Sakamoto, J., Look, K., Lundblad, A., Mattes, M. J., and Lloyd, K. O. (1985) *Biochemistry* **24**, 7820–7826
14. Saito, T., and Hakomori, S. (1971) *J. Lipid Res.* **12**, 257–259
15. Yu, R. K., and Ledeen, R. W. (1972) *J. Lipid Res.* **13**, 680–686
16. Zanetta, J. P., Breckenridge, W. C., and Vincendon, G. (1972) *J. Chromatogr.* **69**, 291–304
17. Warren, L. (1959) *J. Biol. Chem.* **234**, 1971–1975
18. Yu, R. K., and Ledeen, R. W. (1970) *J. Lipid Res.* **11**, 506–510
19. Ando, S., and Yu, R. K. (1977) *J. Biol. Chem.* **252**, 6247–6250
20. Hakomori, S. (1964) *J. Biochem. (Tokyo)* **55**, 205–208
21. Bjorndal, H., Lindberg, B., and Svensson, S. (1970) *Carbohydr. Res.* **15**, 339–349
22. Stellner, K., Saito, H., and Hakomori, S. (1973) *Arch. Biochem. Biophys.* **155**, 464–472
23. Rauvala, H., and Karkkainen, J. (1977) *Carbohydr. Res.* **56**, 1–9
24. Inoue, S., and Matsumura, G. (1979) *Carbohydr. Res.* **74**, 361–368
25. Ando, S., Kon, K., Isobe, M., and Yamakawa, T. (1973) *J. Biochem. (Tokyo)* **73**, 893–895
26. Rauvala, H., Krusius, T., and Finne, J. (1978) *Biochim. Biophys. Acta* **531**, 266–274
27. Chait, B. T., Agosta, W. C., and Field, F. H. (1981) *Mass Spectrom. Ion Phys.* **39**, 339–366
28. Kushi, Y., Handa, S., Kambara, H., and Shizukuishi, K. (1983) *J. Biochem. (Tokyo)* **94**, 1841–1850
29. Carr, S. A., and Reinhold, V. N. (1984) *Biomed. Mass Spectrom.* **11**, 633–642
30. Arita, M., Iwamori, M., Higuchi, T., and Nagai, Y. (1983) *J. Biochem. (Tokyo)* **93**, 319–322
31. Arita, M., Iwamori, M., Higuchi, T., and Nagai, Y. (1984) *J. Biochem. (Tokyo)* **94**, 249–256
32. Arita, M., Iwamori, M., Higuchi, T., and Nagai, Y. (1984) *J. Biochem. (Tokyo)* **95**, 971–981
33. Iwamori, M., Shimoru, J., Tsuyuhara, S., and Nagai, Y. (1984) *J. Biochem. (Tokyo)* **95**, 761–770
34. Egge, H., Peter-Katalinic, J., Reuter, G., Schauer, R., Ghinoni, R., Sonnino, S., and Tettamanti, G. (1985) *Chem. Phys. Lipids* **37**, 127–141
35. Fukuda, M. N., Dell, A., Oates, J. E., Wu, P., Klock, J. C., and Fukuda, M. (1985) *J. Biol. Chem.* **260**, 1067–1082
36. Dell, A. (1987) *Adv. Carbohydr. Chem.* **45**, 19–72
37. Fukuda, M. N., Dell, A., Tiller, P. R., Varki, A., Klock, J. C., and Fukuda, M. (1986) *J. Biol. Chem.* **261**, 2376–2383
38. Mansson, J. E., Mo, H., Egge, H., and Svennerholm, L. (1986) *FEBS Lett.* **196**, 259–262
39. Svennerholm, L. (1963) *J. Neurochem.* **10**, 613–623

Continued on next page.

SUPPLEMENTAL MATERIAL

IDENTIFICATION OF NeuGc-CONTAINING GANGLIOSIDES OF CAT AND SHEEP ERYTHROCYTES. <sup>252</sup>Cf FISSION FRAGMENT IONIZATION MASS SPECTROMETRY IN THE ANALYSIS OF GLYCOSPHINGOLIPIDS

by  
Koichi Furukawa, Brian T. Chait and Kenneth O. Lloyd

A number of model ganglioside of known structure were examined using <sup>252</sup>Cf fission fragment ionization mass spectrometry method. They were (NeuAc)GM1, (NeuAc)GM3, (NeuGc)GM3, and (NeuAc)GD3.

METHODS

Between 1 and 5 nmoles of methylated ganglioside was dissolved in a total of 20ul of methanol:chloroform (1:1) and electrospayed (27) onto a thin aluminized polyester sample support foil with 1 cm<sup>2</sup> of surface area (27). The mass spectrum of the resulting thin solid ganglioside sample film was obtained using a <sup>252</sup>Cf fission fragment ionization time-of-flight mass spectrometer constructed at The Rockefeller University and described previously (27,29).

RESULTS

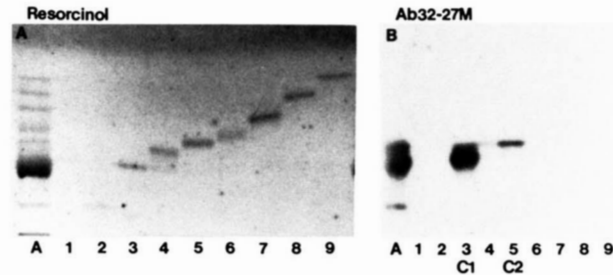


FIG. 1. Purification of cat erythrocyte gangliosides. Panel A: gangliosides fractionated by preparative TLC (resorcinol spray). Lane A: unfractionated sample. Solvent 3 was used. Panel B: immunostaining pattern of the same samples with Ab32-27M (1:8 of hybridoma supernatant). Solvent 2 was used. Fractions 3 and 5, showing Ab-positive bands, were used in subsequent studies and were designated C1 and C2, respectively.

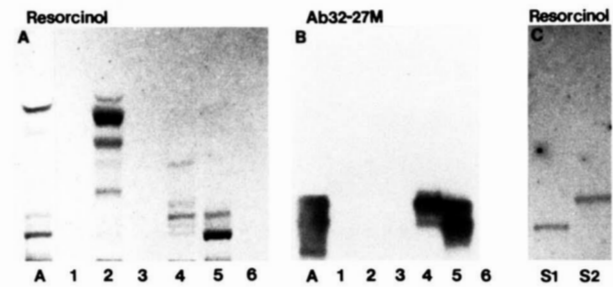


FIG. 2. Purification of sheep erythrocyte gangliosides. Panel A: gangliosides fractionated by step-wise elution from a DEAE-Sephadex column (resorcinol spray). Lane A: unfractionated sample. Fractions 1 - 6 were eluted by C.M:sodium acetate (30:60:8) with increasing concentrations of sodium acetate: 0.05, 0.1, 0.15, 0.2, 0.25, and 0.3M. Solvent 3 was used. Panel B: immunostaining pattern of the same samples as in A with Ab 32-27M (1:8 of hybridoma supernatant). Solvent 2 was used. The components eluted in fractions 4 and 5 were reactive with antibody. Panel C: Two gangliosides purified from fractions 4 and 5 by preparative TLC using solvent. They were designated S1 and S2.

A comparison of the positive ion fission fragment ionization mass spectra obtained from underivatized GM1 and methylated GM1 showed that the mass spectrometric response of the latter was more than two orders of magnitude more intense than the former. In addition, the methylated material yielded a more informative spectrum of fragmentation products than did the underivatized material. For these reasons all of the gangliosides examined in the present study were methylated prior to mass spectrometric analysis.

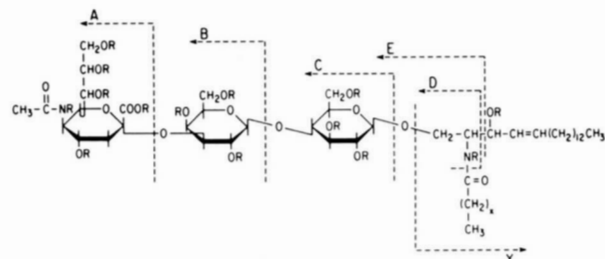


FIG. 16. Structure of (NeuAc)GM3 showing proposed fragmentation pattern in fission fragment ionization mass spectroscopy.

Fig. 15 shows the partial fission fragment time-of-flight mass spectrum of dog erythrocyte (NeuAc)GM3 between m/z (mass-to-charge ratio) 300 and m/z 2300. The positive ion spectrum of GM3 and all of the other gangliosides that we studied were characterized by the presence of relatively intense peaks corresponding to the sodium cationized intact molecule [M + Na]<sup>+</sup> and also by structurally informative and easily interpretable fragmentation products. From the observed ion peaks, the composition of GM3 could be deduced, both in terms of sugar composition as well as the ceramide. The interpretation of the fragmentation pattern of permethylated GM3 is indicated in Fig. 15 with reference to the structure shown in Fig. 16. The masses were determined with sufficient accuracy (250ppm) to allow unambiguous assignment of the nominal masses of the fragment ion. It should be noted, however, that the <sup>252</sup>Cf fission fragment time-of-flight mass spectrometer used in the present study has insufficient resolution to clearly separate adjacent mass peaks above m/z 1000. Thus the m/z values given for all peaks above m/z 1000 are values which are averaged over the unresolved constituent isotopic components as well as over closely related constituent fatty acyl components (e.g. C24:0 and C24:1 in the m/z 1845 peak shown in Fig. 9 for GD3). A particularly significant ion fragment gives rise to the intense peak labelled [A + H<sup>+</sup>-H] at m/z 376 which can be formally accounted for by protonation of the terminal N-acetylneuraminic acid moiety followed by cleavage 'A' and transfer of hydrogen to the neutral fragment. A related ion species at m/z 344 can be accounted for by the additional loss of CH<sub>2</sub>OH from the m/z 376 ion. Three fragment ion peaks yield molecular weight information on the total carbohydrate portion of GM3. The ions with m/z 792 and 776 likely arise by sodium cationization of the carbohydrate portion followed by cleavage 'C' and transfer of OH and OCH<sub>3</sub> respectively. The ion with m/z 879 likely arises by sodium cationization followed by cleavage 'D' of the two arms of the ceramide as indicated. Intense peaks corresponding to the ceramide portion of GM3 are also observed centered about m/z 659 and 661. Detailed inspection of this portion of the mass spectrum (see insert in Fig. 15) indicates considerable heterogeneity in the fatty acyl chain of the ceramide which largely mirrors the heterogeneity observed in the cluster of peaks corresponding to sodium cationized intact GM3.

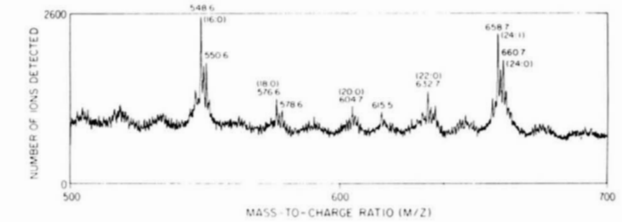


FIG. 17. Uncompressed mass spectrum of methylated GD3 ganglioside in the region between m/z 500-700. The assignment of peaks to different fatty acids in the ceramide moiety are indicated.

The major ion peaks observed at m/z 659 and 661 are consistent with C24:1 and C24:0 fatty acyl chains assuming the long chain base to be 4-sphinganine. Minor peaks were also observed at m/z 645 and 647 and at m/z 673 and 675 which could be attributed to C23 and C25 chains respectively. This interpretation was confirmed by gas chromatographic analysis of the fatty acid composition (data not shown). The additional undersigned peaks in the inset at m/z 660 and m/z 662 are due to <sup>13</sup>C-containing isotopic components. The difference in mass between the most intense [M + Na]<sup>+</sup> ion peaks and the pair of weak fragment ion peaks at m/z 1228 and 1230, which we attribute to cleavage between C2 and C3 of the base (E + Na<sup>+</sup>-H), provides additional confirmation that the base is 4-sphinganine.

Spectra obtained from a sample of (NeuGc)GM3 yielded an analogous series of fragment ion peaks to those described above for the (NeuAc)GM3 except that the carbohydrate-containing fragment masses were, as expected, all 30u higher (data not shown).

As shown in Fig. 9, the mass spectrum of (NeuAc)GD3 (Fig. 8 with R = R<sub>1</sub> = CH<sub>2</sub>CO) was not significantly complicated by the presence of two sialic acid residues. The [M+Na]<sup>+</sup> region of the mass spectrum exhibited a large number of peaks indicating a considerable degree of heterogeneity within the GD3 sample. That this heterogeneity is contained within the ceramide portion of the molecule is implied by the close similarity between the pattern of ceramide fragment ions (Y + H<sup>+</sup>-H) shown in detail in Fig. 17 and that of the [M+Na]<sup>+</sup> ions and also by the absence of any observed heterogeneity with the carbohydrate portion of the molecule. The fatty acid composition of GD3 as deduced from Fig. 17 is compared in Table III with the composition determined from a gas chromatographic analysis of the same sample. In general a reasonable agreement was observed between the two methods. As in the case of GM3, the most intense peaks in the spectrum at m/z 376 and 344 arise from the terminal NeuAc moiety. The disialyl nature of GD3 could be deduced by the characteristic ions at m/z 737 (C + Na<sup>+</sup>-COOR). The ion at m/z 737 arises while that at m/z 717 appears to be formed by sodium ion addition to the disialyl moiety followed by cleavage 'C' and loss of the adjacent COOCH<sub>3</sub> group. Signals at m/z 717 and 737 are absent from the spectra of GM3 so that disialyl gangliosides can be readily distinguished from monosialyl gangliosides using this technique. Indeed, as is seen in the main body of the manuscript, the sequence of sialic acid groups can be directly read off the mass spectrum in disialyl gangliosides where the sialic acid groups are not identical. Ions (D + Na<sup>+</sup>-CH<sub>2</sub>) and (D + Na<sup>+</sup>-OCH<sub>3</sub>) derived from the disialyl-galactose moiety were detected at m/z 1154 and m/z 1139 and a sodium cationized fragment containing the entire carbohydrate portion of the molecule, formed by cleavage 'G' of the two arms of the ceramide was detected at m/z 1241.

The systematic fragmentation behavior of the four known gangliosides described above were employed to elucidate the structures of the four compounds discussed in the main body of the manuscript.

TABLE III

FATTY ACID	MASS SPECTROMETRIC ANALYSIS	GAS CHROMATOGRAPHIC ANALYSIS
14:0	%	5.6 <sup>a</sup>
16:1	7.5	3.8
16:0	24.3	20.0
18:1	2.8	10.8 <sup>a</sup>
18:0	7.1	7.9
20:1	2.8	6.4
20:0	5.8	6.1
22:1	3.7	-
22:0	9.0	7.3
24:1	21.5	19.9
24:0	15.6	12.3

<sup>a</sup>Contain contribution from fatty acids derived from isolation procedures

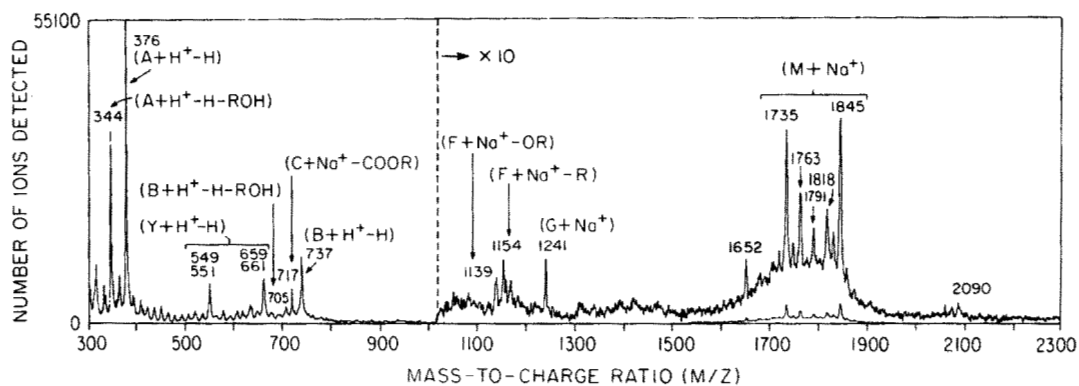


FIG. 9. Partial mass spectrum of methylated (NeuAc)<sub>2</sub>GD<sub>3</sub> shown between m/z 300-2300. M designates the intact molecule. The labels on the fragment ion peaks refer to the fragmentation sites indicated in Fig. 8; R = CH<sub>3</sub>. To allow for convenient representation of the data, the spectrum has been compressed along the mass axis. An uncompressed portion of the spectrum between mass 500-700 is shown in Fig. 17.

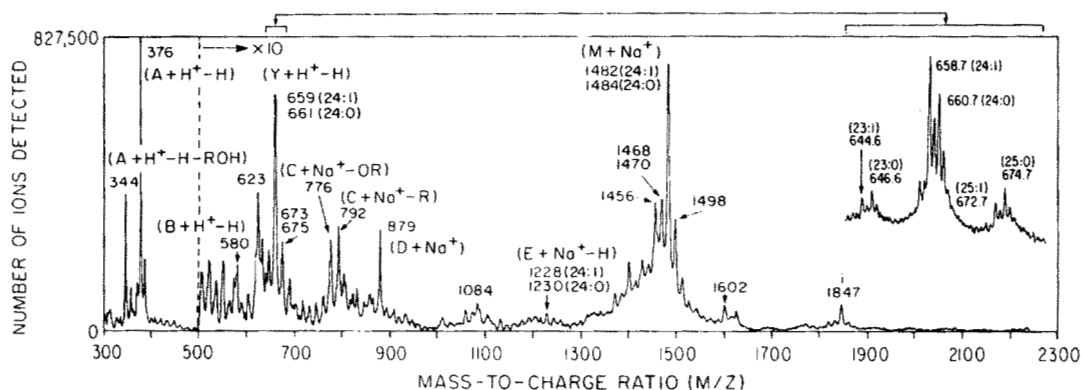


FIG. 15. Partial <sup>252</sup>Cf fission fragment ionization time-of-flight mass spectrum of methylated (NeuAc)GM<sub>3</sub> shown between m/z 300-2300. M designates the intact molecule. The labels on the fragment sites refer to the fragmentation sites indicated in Fig. 16; R = CH<sub>3</sub>. I indicates an ion originating from an impurity. To allow for convenient representation of the data, the spectrum has been compressed along the mass axis. An uncompressed portion of the spectrum showing details of the ceramide fragment ion peaks centered around m/z 659 and 661 is given as an inset; peaks assigned to different fatty acids are indicated. X = 21-23 in Fig. 16.